Comprehensive Lipidomics Analysis of Bioactive Lipids in Complex Regulatory Networks

ARTICLE *in* ANALYTICAL CHEMISTRY · OCTOBER 2010

Impact Factor: 5.64 · DOI: 10.1021/ac1015563 · Source: PubMed

5 AUTHORS, INCLUDING:

Albert Koulman
MRC Human Nutrition Research
65 PUBLICATIONS **1,159** CITATIONS
SEE PROFILE

Dietrich A Volmer
Universität des Saarlandes
203 PUBLICATIONS **2,959** CITATIONS
SEE PROFILE

Anal. Chem. **XXXX,** *xxx,* 000–000

Comprehensive Lipidomics Analysis of Bioactive Lipids in Complex Regulatory Networks

Mojgan Masoodi,[†] Michael Eiden,[†] Albert Koulman,[†] David Spaner,[‡] and Dietrich A. Volmer*[,§]

Elsie Widdowson Laboratory, Medical Research Council, Cambridge, United Kingdom, Division of Molecular and Cellular Biology, Sunnybrook Health Sciences Center, Toronto, Canada, and Institute of Bioanalytical Chemistry, Department of Chemistry, Saarland University, Saarbrücken, Germany

In the present work we describe the development of an analytical technique for simultaneous profiling of over 100 biochemically related lipid mediators in biological samples. A multistep procedure was implemented to extract eicosanoids and other bioactive lipids from the biological matrix, chromatographically separate them using fast reversed-phase liquid chromatography, tentatively identify new candidate eicosanoids through a matching process of retention times, isotope distribution patterns, and high-resolution orbitrap MS/MS fragmentation patterns, and subsequently quantify tentative candidates by means of analytical reference standards. Key new aspects of this profiling technique included the classification of bioactive lipids into 12 groups according to their calculated exact masses and the development of optimized liquid chromatographic conditions for these groups to achieve sufficient separation of the numerous isobaric and isomeric species, many of which exhibited virtually identical collision-induced dissociation behavior. Importantly, no analytical standards were required at this screening stage of the assay, and tentative identifications were achieved by matching results to selected reference species from each of the groups. The analytical figures of merit for the orbitrap assay such as linear dynamic range, limit of detection, limit of quantitation, and precision demonstrated that the performance of the assay was very similar to that of a quadrupole linear ion trap assay, which was used for validation purposes. The method allowed us to examine eicosanoid profiles within the signaling cascade in chronic lymphocytic leukemia (CLL) cells under basal conditions and following arachidonic acid stimulation. The preliminary screening based on high-resolution tandem mass spectrometry data along with isotope pattern and retention time matching revealed the presence of 15 bioactive lipids, belonging to a range of prostaglandin, leukotriene, and hydroxy and epoxy fatty acid lipid mediators produced by CLL cells.

Eicosanoids including prostaglandin, thromboxanes (TXs), leukotrienes (LTs), hydroxyeicosatetranoic acid (HETE), hydroxyeicosapentanoic acid (HEPE), epoxyeicosatrienoic acid (EET), and lipoxins (LXs) are a diverse class of over 100 bioactive lipid mediators derived from arachidonic acid (AA) via cyclooxygenase (COX), lipoxygenase (LOX), and cytochrome P450 (CYP450) as well as nonenzymatic pathways. The COX pathway involves the conversion of AA into prostaglandin H_2 (PGH_2), which is rapidly converted to other prostaglandins (PGD_2, PGE_2, $PGF_{2\alpha}$, and PGI_2) and thromboxane A_2 (TXA_2) by various isomerases. The LOX pathway regulates the conversion of AA to 5-, 12-, or 15-hydroperoxyeicosatetraenoic acid (HpETE), which is metabolized to 5-, 12-, or 15-HETE by 5-, 12-, or 15-LOX, respectively. 15-HETE oxidation by 15-hydroxyprostaglandin dehydrogenase (PGDH) also generates 15-oxo-ETE.[1,2] An alternative pathway for 15-oxo-ETE synthesis proceeds from 15-HpETE.[3] Similarly, 12-lipoxygenase and 5-lipoxygenase have been shown to convert 12-HpETE and 5-HpETE into the corresponding 12- and 5-oxo derivatives.[3−5] HpETE is also converted to leukotriene B4 (LTB_4).[6−8] Furthermore, the lipoxins are also generated from AA via sequential action of two or more LOX enzymes[9] (Scheme 1). Other lipid mediators produced via the LOX pathway include potent anti-inflammatory and proresolving protectins and resolvins derived from eicosapentaenoic acid (EPA, 20:5*n*-3) and docosahexaenoic acid (DHA, 22:6*n*-3), respectively.[9−11] Additionally, LOX metabolizes the 18-carbon linoleic acid (LA) to hydroxyoctadecadienoic acid (HODE).

These lipid autacoids exhibit a large number of physiological and pathophysiological effects in almost every organ system. They have drawn much attention in clinical studies because of their contributions to inflammatory diseases. For example, COX products such as prostaglandins mediate inflammatory response and

* Corresponding author. Phone: +49 681 302 3433. Fax +49 681 302 2963. E-mail: Dietrich.Volmer@mx.uni-saarland.de.

[†] Medical Research Council.

[‡] Sunnybrook Health Sciences Center.

[§] Saarland University.

(1) Bergholte, J. M.; Soberman, R. J.; Hayes, R.; Murphy, R. C.; Okita, R. T. *Arch. Biochem. Biophys.* **1987**, *257*, 444–50.
(2) Wei, C.; Zhu, P.; Shah, S. J.; Blair, I. A. *Mol. Pharmacol.* **2009**, *76*, 516–25.
(3) Fruteau de Laclos, B.; Borgeat, P. *Biochim. Biophys. Acta* **1988**, *958*, 424–33.
(4) Dix, T. A.; Marnett, L. J. *J. Biol. Chem.* **1985**, *260*, 5351–7.
(5) Zarini, S.; Murphy, R. C. *J. Biol. Chem.* **2003**, *278*, 11190–6.
(6) Kuhn, H.; Walther, M.; Kuban, R. J. *Prostaglandins Other Lipid Mediators* **2002**, *68−69*, 263–90.
(7) Radmark, O. *Prostaglandins Other Lipid Mediators* **2002**, *68−69*, 211–34.
(8) Yoshimoto, T.; Takahashi, Y. *Prostaglandins Other Lipid Mediators* **2002**, *68−69*, 245–62.
(9) Serhan, C. N. *Prostaglandins Leukotrienes Essent. Fatty Acids* **2005**, *73*, 141–62.
(10) Bannenberg, G. L.; Chiang, N.; Ariel, A.; Arita, M.; Tjonahen, E.; Gotlinger, K. H.; Hong, S.; Serhan, C. N. *J. Immunol.* **2005**, *174*, 4345–55.
(11) Serhan, C. N.; Savill, J. *Nat. Immunol.* **2005**, *6*, 1191–7.

10.1021/ac1015563

Scheme 1. Arachidonic Acid Cascade

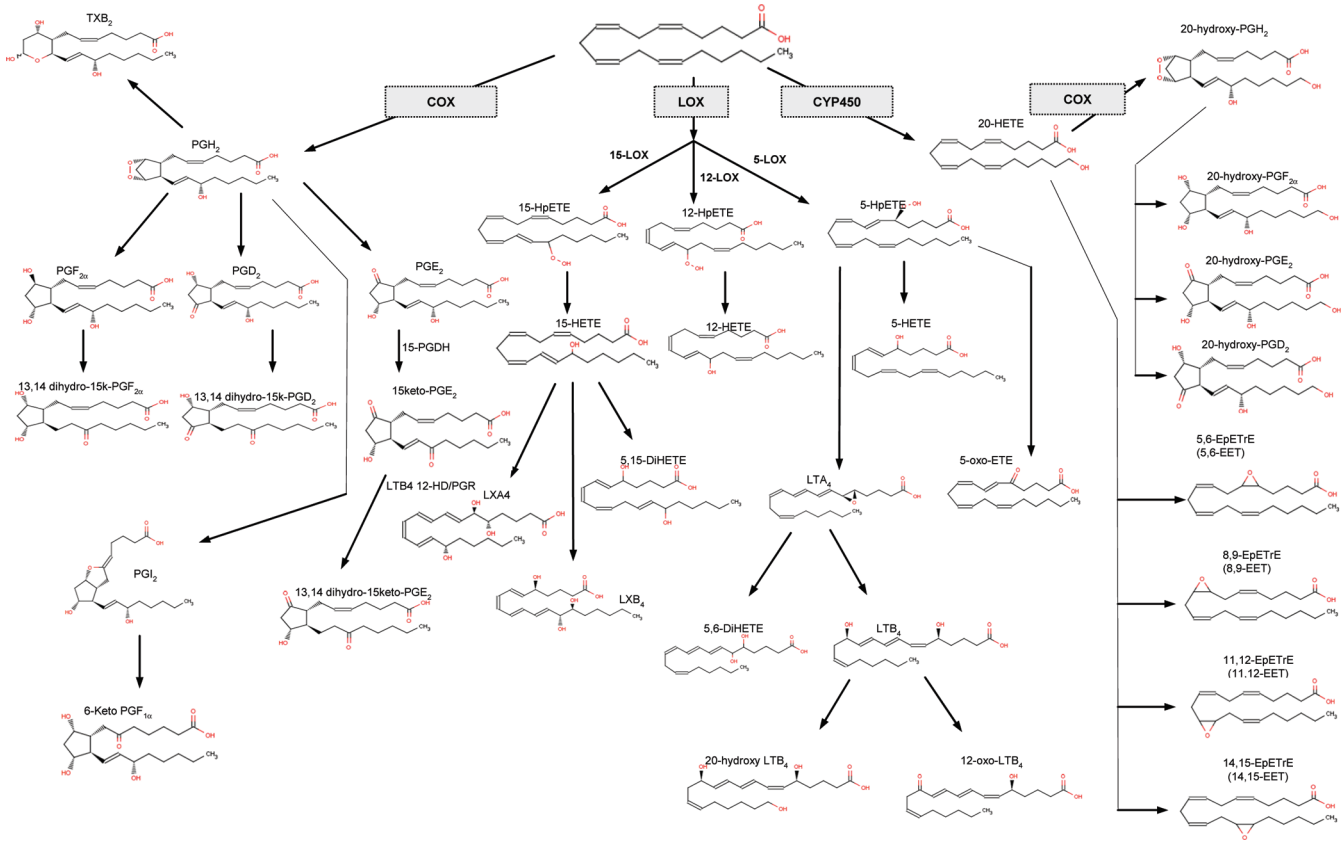

erythema in the skin,[12,13] while CYP450 products such as EETs demonstrate an anti-inflammatory effect by preventing the activation of nuclear factor κB (NF-κB).[14,15] EETs and 20-HETE display multiple biological activities including regulation of blood pressure and cardioprotection,[1,6−18] while LOX metabolites such as 15-HETE and 13-HODE exhibit different effects on cell proliferation and regulating apoptosis.[19−21]

The analytical determination of these metabolites is a challenging task, mainly because of the large number of bioactive lipids that have to be measured to fully characterize the studied biochemical processes. Since these compounds are produced within the same cascade and they all are part of a complex regulatory network, the ideal analytical method would allow the simultaneous profiling and determination of all relevant species in a single analytical assay. This task is further complicated by the presence of a large number of isomers of bioactive lipids with very similar physicochemical properties, existing at very low physiological levels in biological samples. Therefore, a highly sensitive and selective analytical method is required for the comprehensive study of this class of lipids. If successfully implemented, analyzing a large number of these lipid mediators would allow researchers not only to examine the level of individual metabolites, but also to profile lipid mediators across biological systems. Methods currently used include gas chromatography (GC), GC/mass spectrometry (GC/MS), GC/tandem mass spectrometry (GC/MS/MS),[22,23] LC/UV,[24] liquid chromatography/mass spectrometry (LC/MS), and LC/MS/MS.[25−27] LC/MS/MS is currently the most powerful tool for analysis of lipid mediators due to its specificity and sensitivity.[19,25,26,28−31] Several methods have been described in the literature for identification and

(12) Rhodes, L. E.; Gledhill, K.; Masoodi, M.; Haylett, A. K.; Brownrigg, M.; Thody, A. J.; Tobin, D. J.; Nicolaou, A. *FASEB J.* **2009**, *23*, 3947–56.
(13) Tanaka, S.; Sato, T.; Akimoto, N.; Yano, M.; Ito, A. *Biochem. Pharmacol.* **2004**, *68*, 433–9.
(14) Campbell, W. B. *Trends Pharmacol. Sci.* **2000**, *21*, 125–7.
(15) Node, K.; Huo, Y.; Ruan, X.; Yang, B.; Spiecker, M.; Ley, K.; Zeldin, D. C.; Liao, J. K. *Science* **1999**, *285*, 1276–9.
(16) Imig, J. D. *Am. J. Physiol.: Renal. Physiol.* **2005**, *289*, F496–503.
(17) Sarkis, A.; Lopez, B.; Roman, R. J. *Curr. Opin. Nephrol. Hypertens.* **2004**, *13*, 205–14.
(18) Sarkis, A.; Roman, R. J. *Curr. Drug Metab.* **2004**, *5*, 245–56.
(19) Limor, R.; Sharon, O.; Knoll, E.; Many, A.; Weisinger, G.; Stern, N. *Am. J. Hypertens.* **2008**, *21*, 219–23.
(20) Maccarrone, M.; Ranalli, M.; Bellincampi, L.; Salucci, M. L.; Sabatini, S.; Melino, G.; Finazzi-Agro, A. *Biochem. Biophys. Res. Commun.* **2000**, *272*, 345–50.
(21) Shureiqi, I.; Wojno, K. J.; Poore, J. A.; Reddy, R. G.; Moussalli, M. J.; Spindler, S. A.; Greenson, J. K.; Normolle, D.; Hasan, A. A.; Lawrence, T. S.; Brenner, D. E. *Carcinogenesis* **1999**, *20*, 1985–95.
(22) Goulitquer, S.; Dreano, Y.; Berthou, F.; Corcos, L.; Lucas, D. *J. Chromatogr., B Analyt. Technol. Biomed. Life Sci.* **2008**, *876*, 83–8.
(23) Wiswedel, I. *Methods Mol. Biol.* **2009**, *580*, 3–16.
(24) Huang, L. S.; Kang, J. S.; Kim, M. R.; Sok, D. E. *J. Agric. Food Chem.* **2008**, *56*, 1224–32.
(25) Farias, S. E.; Basselin, M.; Chang, L.; Heidenreich, K. A.; Rapoport, S. I.; Murphy, R. C. *J. Lipid Res.* **2008**, *49*, 1990–2000.
(26) Golovko, M. Y.; Murphy, E. J. *J. Lipid Res.* **2008**, *49*, 893–902.
(27) Lawson, J. A.; Kim, S.; Powell, W. S.; FitzGerald, G. A.; Rokach, J. *J. Lipid Res.* **2006**, *47*, 2515–24.
(28) Lee, S. H.; Blair, I. A. *BMB Rep.* **2009**, *42*, 401–10.
(29) Masoodi, M.; Mir, A. A.; Petasis, N. A.; Serhan, C. N.; Nicolaou, A. *Rapid Commun. Mass Spectrom.* **2008**, *22*, 75–83.
(30) Masoodi, M.; Nicolaou, A. *Rapid Commun. Mass Spectrom.* **2006**, *20*, 3023–9.
(31) Oe, T.; Ackermann, B. L.; Inoue, K.; Berna, M. J.; Garner, C. O.; Gelfanova, V.; Dean, R. A.; Siemers, E. R.; Holtzman, D. M.; Farlow, M. R.; Blair, I. A. *Rapid Commun. Mass Spectrom.* **2006**, *20*, 3723–35.

quantification of CYP450 metabolites,[32] selected LOX metabolites,[33] prostaglandins,[34] isoprostanes,[35] and HETEs[36] in a variety of biological matrixes. For example, Kempen et al.[37] reported an LC/MS/MS assay for quantitative analysis of PGE_2 and 11-, 12-, and 5-HETEs from cultured cells. Yue et al. developed a tandem mass spectrometry method allowing simultaneous analysis of 19 eicosanoids including selected LOX, COX, and CYP450 metabolites.[38] We previously described LC/MS/MS analysis of prostaglandins,[30] CYP450, and LOX metabolites.[29] Although these assays are sensitive and selective and cover a large number of metabolites of related pathways, they are limited to the simultaneous analysis of only a limited number of eicosanoids. This limitation is the direct result of a trade-off between analyzing the highest possible number of relevant metabolites and the decreasing sensitivity observed with increasing numbers of monitored compounds. Recently, Yang et al. reported the simultaneous quantitative profiling of 39 COX, LOX, and CYP450 metabolites,[39] reaching almost 40% of the currently known number of eicosanoids (http://www.lipidmaps.org). Unfortunately, important metabolites such as dihydroprostaglandins (e.g., 13,14-dihydro-15-keto-$PGF_{2\alpha}$, a deactivated metabolite of $PGF_{2\alpha}$) or 8-iso-$PGF_{2\alpha}$, a prostaglandin-like metabolite generated from a nonenzymatic pathway, as well as many other related metabolites of the arachidonic acid cascade were not included in the assay.

The aim of the present study was to develop and apply a comprehensive analytical assay that allows for simultaneous profiling of a very large number (>100) of eicosanoids using a single analytical method. To achieve this goal, a multistep procedure was implemented: eicosanoids were initially extracted from the biological matrix and separated using reversed-phase liquid chromatography. For the screening stage, eicosanoids and related bioactive lipids (e.g., metabolites of LA and EPA/DHA) within the cascade were classified into 12 groups on the basis of their calculated exact masses (Table 1). After retention times, isotope distribution patterns, and MS/MS fragmentation spectra were matched, tentatively identified lipid species were subsequently quantified with the aid of analytical reference standards.

To demonstrate the applicability of our approach, we applied this new methodology to the profiling of eicosanoids and other bioactive lipids within the cascade in chronic lymphocytic leukemia (CLL) cells. CLL, a malignancy of activated human B cells, is the most common leukemia in the developed world.[40] It is incurable with conventional therapies, and a better understanding of the biology of this disease is required to improve patient

Table 1. Classification of Eicosanoids and Other Bioactive Lipids Produced via the LOX Pathway Based on Their Calculated Exact Masses

$C_{18}H_{31}O_3$, 296.2134	$C_{20}H_{30}O_3$, 318.2195	$C_{20}H_{32}O_3$, 320.235	$C_{20}H_{30}O_4$, 334.2144	$C_{20}H_{32}O_4$, 336.220	$C_{20}H_{34}O_4$, 338.246	$C_{22}H_{32}O_3$, 344.235	$C_{20}H_{30}O_5$, 350.2093	$C_{20}H_{32}O_5$, 352.2144	$C_{20}H_{34}O_5$, 354.2134	$C_{20}H_{34}O_6$, 370.2355	$C_{22}H_{32}O_5$, 376.225
9-HODE	5(6)-EpETE	5-HETE	PGB_2	5,6-DiHETE	5,6-DiHETrE	17-HDHA	8-iso-15-keto PGE_2	13,14-dihydro-15-keto-PGD_2	13,14-dihydro-15 keto-$PGF_{2\alpha}$	6-keto-$PGF_{1\alpha}$	resolvin D1
13-HODE	8(9)-EpETE	8-HETE	PGJ_2	5,15-DiHETE	8,9-DiHETrE	4-HDoHE	19-hydroxy-PGB_2	13,14-dihydro-15-keto-PGE_2	PGD_1	TXB_2	resolvin D2
	11(12)-EpETE	9-HETE	Δ^{12}-PGJ_2	8,15-DiHETE	11,12-DiHETrE	7-HDoHE	15-keto-PGE_2	13,14-dihydro-15-keto-$PGF_{2\alpha}$	PGE_1	19-hydroxy-$PGF_{2\alpha}$	resolvin D3
	14(15)-EpETE	11-HETE	15-deoxy-$\Delta^{12,14}$-PGD_2	8-HpETE	14,15-DiHETrE	8-HDoHE	PGD_3	8-iso- 15-keto $PGF_{2\alpha}$	8-iso-$PGF_{2\alpha}$	20-hydroxy-$PGF_{2\alpha}$	resolvin D4
	17(18)-EpETE	12-HETE	5-HpETE	9-HpETE		11-HDoHE	PGE_3	20-hydroxy-LTB_4	$PGF_{2\alpha}$	19-hydroxy-PGE_1	
	5-HEPE	15-HETE	12-HpEPE	11-HpETE		13-HDoHE	resolvin E1	15 keto-$PGF_{2\alpha}$	15-keto-$PGF_{1\alpha}$		
	8-HEPE	15-HETE	15-HpEPE	12-HpETE		14-HDoHE		$PGF_{3\alpha}$	8-iso-PGE_1		
	9-HEPE	16-HETE	12-oxo-LTB_4	15-HpETE		16-HDoHE		PGD_2	8-iso-13,14-dihydro-15-keto-$PGF_{2\alpha}$		
	11-HEPE	18-HETE	13,14-dihydro-LTB_4	5,15-DHETE		17-HDoHE		PGE_2			
	12-HEPE	19-HETE		11,12-DHETE		20-HDoHE		lipoxin B4			
	15-HEPE	20-HETE		8,15-DHETE		7(8)-EpDPE		Δ^{12}-PGD_2			
	18-HEPE	5,6-EpETrE		8,9-DHETE		10(11)-EpDPE		Δ^{17}-PGE_1			
	5-oxo-ETE	8,9-EpETrE		14,15-DHETE		13(14)-EpDPE		15-keto-PGE_1			
	12-oxo-ETE	11,12-EpETrE		17,18-DHETE		16(17)-EpDPE		5,6- lipoxin A4			
	15-oxo-ETE	14,15-EpETrE		LTB_4		19(20)-EpDPE		8-iso- $PGF_{3\alpha}$			
				PGB_1							

(32) Nithipatikom, K.; Grall, A. J.; Holmes, B. B.; Harder, D. R.; Falck, J. R.; Campbell, W. B. *Anal. Biochem.* **2001**, *298*, 327–36.

(33) Zhang, J. H.; Pearson, T.; Matharoo-Ball, B.; Ortori, C. A.; Warren, A. Y.; Khan, R.; Barrett, D. A. *Anal. Biochem.* **2007**, *365*, 40–51.

(34) Hishinuma, T.; Suzuki, K.; Saito, M.; Yamaguchi, H.; Suzuki, N.; Tomioka, Y.; Kaneko, I.; Ono, M.; Goto, J. *Prostaglandins Leukotrienes Essent. Fatty Acids* **2007**, *76*, 321–9.

(35) Yan, W.; Byrd, G. D.; Ogden, M. W. *J. Lipid Res.* **2007**, *48*, 1607–17.

(36) Yoshida, Y.; Kodai, S.; Takemura, S.; Minamiyama, Y.; Niki, E. *Anal. Biochem.* **2008**, *379*, 105–15.

(37) Kempen, E. C.; Yang, P.; Felix, E.; Madden, T.; Newman, R. A. *Anal. Biochem.* **2001**, *297*, 183–90.

(38) Yue, H.; Jansen, S. A.; Strauss, K. I.; Borenstein, M. R.; Barbe, M. F.; Rossi, L. J.; Murphy, E. *J. Pharm. Biomed. Anal.* **2007**, *43*, 1122–34.

(39) Yang, J.; Schmelzer, K.; Georgi, K.; Hammock, B. D. *Anal. Chem.* **2009**, *81*, 8085–93.

(40) Caligaris-Cappio, F.; Ghia, P. *J. Clin. Oncol.* **2008**, *26*, 4497–503.

outcomes. Growth of CLL cells appears to depend on the presence of a lipid-rich microenvironment. It has been reported that B cells produce prostaglandin E_2 and LTB_4, which affect proliferation and apoptosis in vitro.[40,41] However, the detailed characterization of intracellular and extracellular pools of related lipid mediators and their role in cell survival is lacking due to limitations in analytical methodology.[42]

Here we present an automated, data-dependent lipidomics assay for investigating the profile of eicosanoids and other related bioactive lipids in CLL cells. This assay provides a comprehensive lipidomics platform for identification of potential lipid mediators in relation to disease pathology and may facilitate the therapeutic approaches.

EXPERIMENTAL SECTION

Chemicals. Prostaglandin D_2 (PGD_2), prostaglandin E_2 (PGE_2), thromboxane B_2 (TXB_2), 6-keto-prostaglandin $F_{1\alpha}$ (6-keto-$PGF_{1\alpha}$), 15-deoxy-$\Delta^{12,14}$-prostaglandin J_2 (15-deoxy-$\Delta^{12,14}$-PGJ_2), 8-iso-$PGF_{2\alpha}$, prostaglandin D_3 (PGD_3), prostaglandin E_3 (PGE_3), prostaglandin B_2-d_4 (PGB_2-d_4), 13,14-dihydro-15-keto-$PGF_{2\alpha}$, 13,14-dihydro-15-keto-PGE_2, 9-hydroxy-10(*E*),12(*Z*)-octadecadienoic acid (9-HODE), 13-hydroxy-9(*Z*),11(*E*)-octadecadienoic acid (13-HODE), 5-hydroxy-6(*E*),8(*Z*),11(*Z*),14(*Z*)-eicosatetraenoic acid (5-HETE), 8-hydroxy-5(*Z*),9(*E*),11(*Z*),14(*Z*)-eicosatetraenoic acid (8-HETE), 11-hydroxy-5(*Z*),8(*Z*),12(*E*),14(*Z*)-eicosatetraenoic acid (11-HETE), 12(*S*)-hydroxy-5(*Z*),8(*Z*),10(*E*),14(*Z*)-eicosatetraenoic-*5,6,8,9,11,12,14,15*-d_8 acid (12-HETE-d_8), 9-hydroxy-5(*Z*),7(*E*),11(*Z*),14(*Z*)-eicosatetraenoic acid (9-HETE), 15-hydroxy-5(*Z*),8(*Z*),11(*Z*),13(*E*)-eicosatetraenoic acid (15-HETE), 12-hydroxy-5(*Z*),8(*Z*),10(*E*),14(*Z*)-eicosatetraenoic acid (12-HETE), 20-hydroxy-5(*Z*),8(*Z*),11(*Z*),14(*Z*)-eicosatetraenoic acid (20-HETE), 18-hydroxy-5(*Z*),8(*Z*),11(*Z*),14(*Z*)-eicosatetraenoic acid (18-HETE), 8(9)-epoxy-5(*Z*),11(*Z*),14(*Z*)-eicosatrienoic acid (8,9-EET), 11(12)-epoxy-5(*Z*),8(*Z*),14(*Z*)-eicosatrienoic acid (11,12-EET), 14(15)-epoxy-5(*Z*),8(*Z*),11(*Z*)-eicosatrienoic acid (14,15-EET), 17-hydroxy-4(*Z*),7(*Z*),10(*Z*),13(*Z*),15(*E*),19(*Z*)-docosahexaenoic acid (17-HDoHE), 10(*S*),17(*S*)-dihydroxy-4(*Z*),7(*Z*),11(*E*),13(*Z*),15(*E*),19(*Z*)-docosahexaenoic acid (17(*S*)-DiHDoHE), leukotriene B4 (LTB_4), and arachidonic acid were purchased from Cayman Chemicals (Ann Arbor, MI). HPLC-grade acetonitrile, ethanol, methanol, hexane, and hydrochloric acid were from Fisher Chemicals (Loughborough, U.K.), HPLC-grade glacial acetic acid and methyl formate from Sigma (Dorset, U.K.), and solid-phase extraction (SPE) cartridges (C_{18}-E, 500 mg, 6 mL) from Phenomenex (Macclesfield, U.K.).

CLL Cells. Heparinized blood was collected from otherwise untreated, consenting CLL patients (diagnosed by a persistent monoclonal expansion of CD19 + CD5 + IgMlo lymphocytes[43] with approval by the Sunnybrook Review Board). CLL cells were isolated as previously described[44] by negative selection with the Rosette Sep human B cell enrichment cocktail (StemCell Technologies, Vancouver, BC) and density centrifugation with Ficoll-Paque (Amersham Pharmacia Biotech AB, Uppsala, Sweden). This method of purification yields percentages of $CD19^+$ and $CD19^+/CD5^+$ cells of >98% and 96%, respectively.[44]

Cell Culture and Activation. Purified CLL cells (2×10^6 per mL) were cultured in 6 mL of Invitrogen RPMI 1640 (Burlington, ON) plus 1 μg/mL insulin (Humulin R, Eli Lilly, Toronto, ON), 5 μg/mL transferrin (Sigma), 2 mM glutamine (Wisent Bioproducts, St-Bruno, QC), and 1% fraction V bovine serum albumin (BSA) (Sigma). The cells were treated with 10 μM AA. Albumin-bound AA was prepared by stirring the fatty acid sodium salt at 37 °C with 5% BSA and added to the serum-free culture medium at a final concentration of 1% BSA. Supernatants from the control and arachidonic acid-challenged culture were collected after 24 h. To assess the levels of metabolites produced as a result of AA autoxidation during a 24 h incubation period, a negative control sample was prepared, where AA was added to cell culture media only and incubated for 24 h.

Solid-Phase Extraction. The procedure was performed using a vacuum manifold (Phenomenex) as described previously.[29,30] Briefly, cell culture media (6 mL) were collected and adjusted to 15% methanol (v/v). Internal standard PGE_2-d_4 and 12-HETE-d_8 (40 ng) were added to each sample. The samples were acidified with 0.05 M hydrochloric acid to pH 3.0 and immediately applied to SPE cartridges that had been preconditioned with 20 mL of methanol, followed by 20 mL of water. The cartridges were then washed with 20 mL of 15% (v/v) methanol, 20 mL of water, and 10 mL of hexane. Finally, the eicosanoids were eluted with 15 mL of methyl formate. The organic solvent was evaporated using a fine stream of nitrogen, the remaining residue redissolved in ethanol (100 μL), and the final solution stored at −20 °C prior to analysis.

LC/MS/MS Analysis. Chromatographic analyses were performed using Accela UHPLC (Thermo Scientific, Hemel Hempstead, U.K.) and Acquity UPLC (Waters, Hertsfordshire, U.K.) systems. The bioactive lipids were separated on a C_{18} reversed-phase (RP) LC column (Phenomenex Luna, 3 μm particles, 150 × 2 mm) using a linear mobile phase gradient (A, 0.02% glacial acetic acid in water; B, 0.02% glacial acetic acid in acetonitrile) at 0.7 mL/min. The starting conditions consisted of 30% B and were maintained for 1 min. The gradient then increased to 90% B over 12 min and finally returned to the initial conditions for 2 min to allow equilibration. For automated peak-picking in sample chromatograms, a retention time window of ±10 s relative to t_R of the corresponding calibration standard was set. In addition, to improve accuracy, the retention data were normalized to the internal standards. Mass spectrometry analyses were carried out on LTQ Velos (Thermo, Hemel Hempstead, U.K.) linear ion trap (LIT)−orbitrap and QTRAP 4000 (AB Sciex, Concord, ON) quadrupole−linear ion trap (QqLIT) mass spectrometers. The analyses on the orbitrap instrument were performed using heated electrospray ionization (h-ESI) in negative ion mode at sheath, auxiliary, and sweep gas flows of 24, 10, and 5, respectively. The capillary and source heater temperatures were set to 325 and 50 °C, respectively. The ion spray voltage was adjusted to 4000 V. Resolving powers of 30 000 in full scan mode and 7500 in MS/MS mode were used. The QTRAP analyses were conducted in negative ion mode under multiple reaction monitoring (MRM)

(41) Kay, N. E.; O'Brien, S. M.; Pettitt, A. R.; Stilgenbauer, S. *Leukemia* **2007**, *21*, 1885–91.
(42) Runarsson, G.; Liu, A.; Mahshid, Y.; Feltenmark, S.; Pettersson, A.; Klein, E.; Bjorkholm, M.; Claesson, H. E. *Blood* **2005**, *105*, 1274–9.
(43) Spaner, D. E.; Shi, Y.; White, D.; Shaha, S.; He, L.; Masellis, A.; Wong, K.; Gorczynski, R. *Leukemia* **2010**, *24*, 222–6.
(44) Gitelson, E.; Hammond, C.; Mena, J.; Lorenzo, M.; Buckstein, R.; Berinstein, N. L.; Imrie, K.; Spaner, D. E. *Clin. Cancer Res.* **2003**, *9*, 1656–65.

conditions. The turbospray temperature was set to 300 °C, the curtain gas flow to 25 psi, and the ion spray voltage to 4000 V. The collision energy (CE), desolvation potential (DP), and collision cell exit potential (CXP) were optimized for each compound (see the Supporting Information).

For automated data processing, data acquisition files were converted to the *.mzXML standard and analyses were carried out using the open-source Bioconductor packages XCMS (version 1.22.1)[45] and CAMERA (version 1.4.2).

Recovery Experiments from Biological Samples. The sample recoveries were determined similarly to a previous procedure.[29,30] Briefly, RPMI cell culture media (10 mL) were spiked with an eicosanoid standard mixture containing one selected metabolite per class (Table 1) at 20 ng/eicosanoid (see the subsection "Calibration Experiments" below). The metabolites were extracted from spiked and nonspiked samples and the estimated recoveries calculated as follows:

$$\text{recovery} = ((\text{extracted spiked} - \text{extracted nonspiked})/\text{nonextracted standards}) \times 100$$

Calibration Experiments. For method development and screening purposes a mixture of representative compounds from each class (Table 1), including 5-oxo-ETE, 11-HETE, PGB_2, LTB_4, PGE_3, PGE_2, $PGF_{2\alpha}$, TXB_2, 15-deoxy-$\Delta^{12,14}$-PGJ_2, 17-HDHA, RvD_2, and 13-HODE, was prepared and used as a calibration standard. For quantitative analysis of CLL cells, the tentatively identified compounds were additionally included in the mixture. The mixture was prepared in ethanol at a final concentration of 10 ng/μL, sealed under nitrogen, and stored at −20 °C. Calibration solutions were prepared by mixing and diluting the appropriate stock solutions and adding internal standards to the final concentration of 1000, 500, 200, 80, 40, 20, and 10 pg/μL. The calibration curves were calculated using least-squares linear regression.

Method Validation. Six batches of calibration solutions were used to determine limits of detection (LODs), limits of quantitation (LOQs), precision, linearity, inter- and intraday mass accuracy, method accuracy, and recovery for the lipidomics assay. The precisions were expressed as relative standard deviations (RSDs). The LODs were estimated by using signal-to-noise (S/N) ratios of 3. The limit of quantitation (LOQ) was defined as the concentration value above which the measured precisions were ≤15% RSD. Method accuracies were calculated as the percent deviation from the nominal concentrations. Samples were analyzed on LTQ Velos orbitrap and QqLIT mass spectrometers. The measured mass accuracies for the orbitrap instrument were <3 ppm in all experiments using external m/z calibration. The inter- and intraday mass accuracies for MS and MS/MS experiments were determined using six batches of the mixed standards and checked for all the detected compounds in biological samples.

RESULTS AND DISCUSSION

Profiling and quantitative analysis of eicosanoids and their metabolites in biological samples require robust, precise, accurate, and sensitive analytical methodologies. As eicosanoids possess free carboxylic acid groups, electrospray ionization (ESI) in the negative ion mode can be readily used to generate abundant $[M - H]^-$ carboxylate precursor ions, allowing analyses at low concentration levels. The response behavior across the various investigated lipid mediators differed somewhat in the negative ionization mode for many of the investigated compounds. In our experiments, relative response factors for 24 selected eicosanoids varied between 67% and 251% for the $[M - H]^-$ precursor ion (relative to an arbitrary standard compound, LTB_4; see Table 2), with only 4 compounds outside a range of 50−200% of the reference compound. This variation was higher when a structurally characteristic product ion in MS/MS experiments was used instead of the precursor ion, viz., between 20% and 314%, reflecting the additional influence of variations of product ion abundances (Table 2).

Despite the high ionization efficiency, analysis is challenging for several reasons. First, a large number of isomeric and isobaric eicosanoid species exist, which require a high resolving power, both at the separation and at the tandem mass spectrometry (MS/MS) stage. Several eicosanoid isomers exhibit identical or virtually identical fragmentation patterns, necessitating the use of high-resolution liquid chromatography for their separation. Equally, the remaining coeluting isobaric and isomeric species require high-resolution MS/MS analysis to distinguish them. There are several reports in the literature on the use of triple-quadrupole (QqQ) mass spectrometry in the MRM mode for quantitation of eicosanoids.[19,25,26,29−31] While using a QqQ instrument in the MRM mode has been shown to be highly sensitive and selective,

Table 2. Relative Response Factors (R/R_0), Linearity, Correlation Coefficient (r), Limits of Detection (LODs), and Accuracy of the LC/ESI-MS/MS Assay for Eicosanoids Using Orbitrap Mass Spectrometry[a]

lipid	MW	R/R_0 (MS)	R/R_0 (MS/MS)	LOD (pg)	r^2	accuracy (%)
TXB_2	370.5	0.99 ± 0.10	0.77 ± 0.10	10	0.9979	97
6-keto-$PGF_{1\alpha}$	370.5	1.56 ± 0.10	0.86 ± 0.07	10	0.9967	95
PGE_2	352.5	0.91 ± 0.09	1.18 ± 0.13	10	0.9989	98
13-HODE	296.5	1.88 ± 0.06	0.20 ± 0.01	10	0.9962	96
9-HODE	296.5	1.88 ± 0.06	0.24 ± 0.01	10	0.9981	96
PGE_3	350.5	0.67 ± 0.06	0.77 ± 0.03	20	0.9967	95
PGD_2	352.5	0.74 ± 0.12	0.32 ± 0.11	20	0.9724	95
13,14-PGE_2	352.5	0.92 ± 0.04	0.70 ± 0.18	20	0.9992	98
8-iso-$PGF_{2\alpha}$	354.5	1.38 ± 0.27	0.61 ± 0.07	10	0.9990	103
11,12-EET	320.5	2.09 ± 0.09	0.98 ± 0.04	10	0.9997	96
8,9-EET	320.5	2.46 ± 0.26	0.45 ± 0.01	10	0.9981	98
$PGF_{2\alpha}$	354.5	2.51 ± 0.29	1.20 ± 0.07	10	0.9952	98
14,15-EET	320.5	2.36 ± 0.26	0.39 ± 0.01	10	0.9976	103
13,14-$PGF_{2\alpha}$	354.5	1.18 ± 0.09	1.20 ± 0.10	20	0.9956	97
LTB_4[b]	336.5	1.00 ± 0.00	1.00 ± 0.00	10	0.9989	99
5-HETE	320.5	1.60 ± 0.16	0.96 ± 0.05	10	0.9995	97
8-HETE	320.5	1.70 ± 0.30	0.88 ± 0.13	10	0.9859	97
9-HETE	320.5	2.00 ± 0.04	0.31 ± 0.02	30	0.9875	98
11-HETE	320.5	2.06 ± 0.04	3.14 ± 0.13	10	0.9982	94
12-HETE	320.5	1.75 ± 0.04	0.42 ± 0.01	20	0.9899	96
20-HETE	320.5	1.81 ± 0.13	0.29 ± 0.02	30	0.9984	95
18-HETE	320.5	1.41 ± 0.56	0.94 ± 0.01	10	0.9954	101
15-HETE	320.5	1.97 ± 0.09	0.34 ± 0.01	10	0.9999	95
PGB_2	334.5	0.74 ± 0.05	0.45 ± 0.11	10	0.9932	98

[a] LODs are expressed as picograms injected on-column resulting in an S/N ratio of ∼3:1. The relative signal intensities R/R_0 are expressed using equimolar amounts of lipids and are calculated for MS data from extracted ion chromatograms of full scan (MS) and product ion chromatograms (MS/MS). The data represent the mean ± standard deviation (SD) (n = 3 experiments). [b] LTB_4 was selected as a reference (R_0).

(45) Smith, C. A.; Want, E. J.; O'Maille, G.; Abagyan, R.; Siuzdak, G. *Anal. Chem.* **2006**, *78*, 779–87.

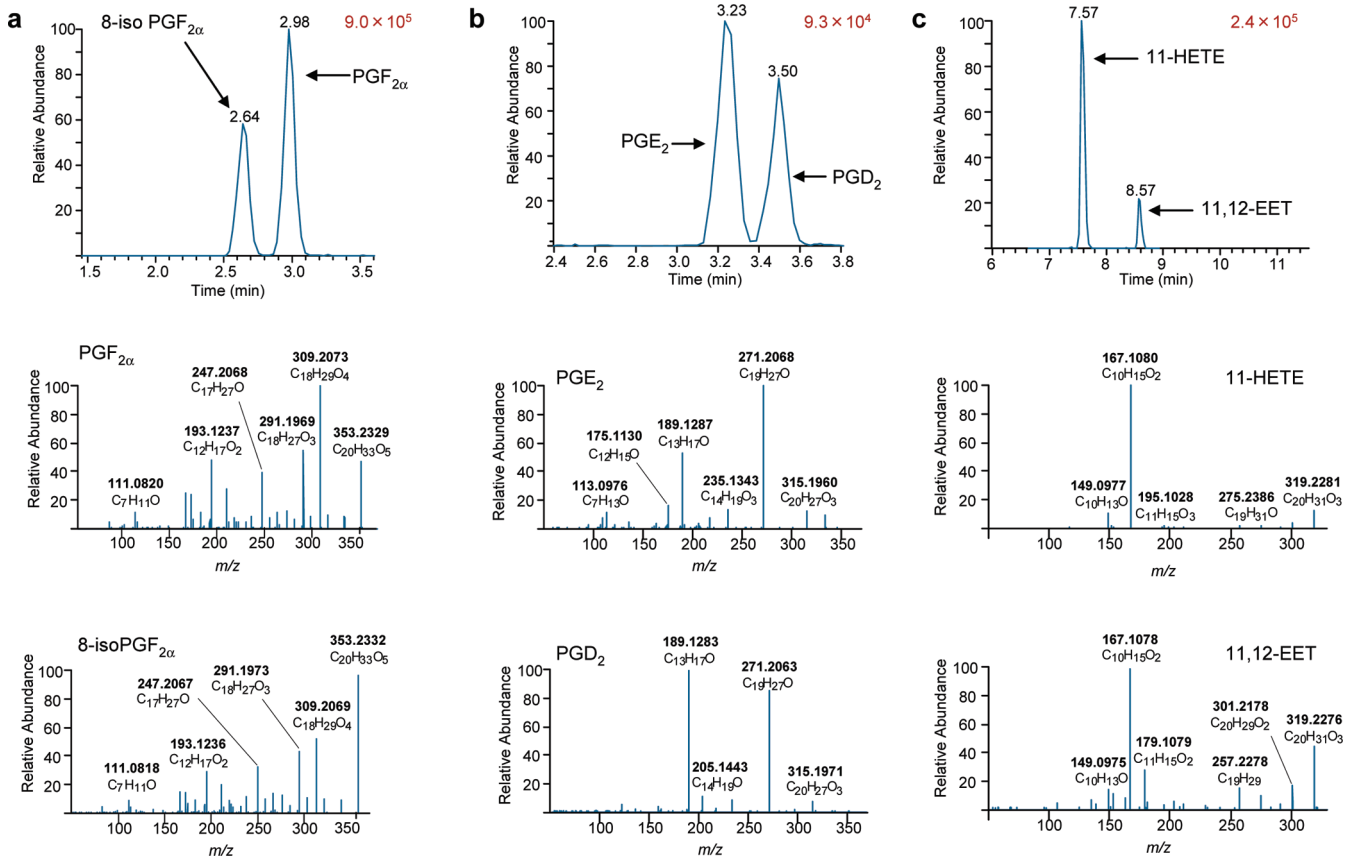

Figure 1. Orbitrap high-resolution extracted ion chromatograms illustrating successful separation of three critical pairs (top): (a) $PGF_{2\alpha}$/8-iso-$PGF_{2\alpha}$, (b) PGE_2/PGD_2, and (c) 11-HETE/11,12-EET. The bottom spectra show the virtually identical MS/MS spectra for each of these isomer pairs.

it is limited to target analysis of selected compounds. A QqQ approach also requires careful optimization of every MRM transition and thus necessitates costly analytical standards. Increasing the number of MRM transitions to include more species will reduce the sensitivity, in particular when the number of investigated compounds is very large, as was the case in this study (>100 eicosanoid species). It has been recently shown, however, that modern QqQ instruments are readily able to conduct MRM experiments with a very large number of MRM transitions. For example, Lopez et al. demonstrate the use of 193 MRM transitions to analyze peptides at the 1−5 fmol range.[46]

In this study, we have developed an automated, data-dependent assay to simultaneously screen for over 100 bioactive lipids in biological samples, using a single electrospray mass spectrometry assay. The assay's targeted application range was the entire biochemical cascade as outlined in Scheme 1. The implemented analytical strategy consisted of a four-step procedure: (1) extraction of lipids from the biological matrix and UHPLC separation/high-resolution MS analysis; (2) screening of sample extracts without analytical standards using the predicted ion lists and exact mass filtering; (3) tentative compound identification by matching theoretical MS/MS product ion patterns, retention times, and isotope patterns with measured data; (4) final confirmation and quantitation of candidates using reference standards. Importantly, quantification was also conducted using the orbitrap mass spectrometer, after the quantitative assay was carefully correlated and validated with a corresponding triple-quadrupole MRM method.

Data-Dependent Acquisition Protocol and Compound Identification Process. For the screening stage of the assay, the eicosanoids and the related bioactive lipids were initially classified into 12 groups according to their calculated exact masses. The liquid chromatography method was specifically optimized to achieve sufficient separation of the numerous isobaric and isomeric species within each of these groups (see Table 1). This is demonstrated exemplarily by means of three isomeric lipid pairs, viz., $PGF_{2\alpha}$/8-iso-$PGF_{2\alpha}$, PGE_2/PGD_2, and 12-HETE/11,12-EET. These pairs exhibit identical exact masses ($C_{20}H_{34}O_5$, $C_{20}H_{32}O_5$, and $C_{20}H_{32}O_3$ at m/z 353.2334, 351.2177, and 319.2278, respectively), very similar dissociation behavior under collision-induced dissociation (CID) conditions, and, if not optimized, very similar chromatographic retention. Figure 1 shows the results of the optimization process and illustrates the well-resolved exemplary isomeric lipid pairs.

The m/z ratios of the 12 groups were subsequently used for an inclusion list in data-dependent tandem mass spectrometry experiments. In these screening experiments, a full scan mass spectrum and MS/MS spectra of the five most intense ions from the inclusion list were acquired, thus allowing coeluting compounds with different m/z ratios to be selected and made to undergo CID in the orbitrap mass spectrometer. Collision activation can be performed in two collision regions of the orbitrap instrument, the LIT and the so-called "higher energy collision

(46) Lopez, M. F.; Kuppusamy, R.; Sarracino, D. A.; Prakash, A.; Athanas, M.; Krastins, B.; Rezai, T.; Sutton, J. N.; Peterman, S.; Nicolaides, K. *J. Proteome Res.*, in press.

dissociation (HCD)" cell. The HCD cell provides triple-quadrupole-like CID spectra and was used in most experiments in this study. Importantly, in these experiments the m/z windows were adjusted to within a 10 ppm tolerance, to avoid fragmentation of undesired interfering compounds.

The orbitrap CID spectra of the investigated lipid species exhibited characteristic fragmentation patterns. For example, abundant fragment ions at $[M - H - H_2O]^-$, $[M - H - 2H_2O]^-$, $[M - H - H_2O - CO_2]^-$, and $[M - H - 2H_2O - CO_2]^-$ were observed for eicosanoids such as PGE_2, PGD_2, PGE_3, and 15-keto-PGE_2 depending on the number of hydroxy group as reported previously.[47−49] In addition, α-hydroxy cleavage has been suggested as the underlying mechanism for production of abundant fragment ions seen with other eicosanoids such as LTB_4, $PGF_{2\alpha}$, and 8-iso-$PGF_{2\alpha}$,[50−52] e.g., PGE_2/PGD_2 at m/z 333 ($[M - H - H_2O]^-$), m/z 315 ($[M - H - 2H_2O]^-$), and m/z 271 ($[M - H - 2H_2O - CO_2]^-$).

Generally, structural differences between HETEs are due to the location of hydroxy groups. For instance, 5-HETE and 12-HETE both feature a hydroxyl group at the C-5 and C-12 positions, respectively. The location of this hydroxy group and its relative distance to nearby double bonds determine the formation of product ions formed in the CID process. Not surprisingly, the fragmentation patterns were slightly different between the two collision regions of the orbitrap instrument. CID in the linear ion trap primarily resulted in $[M - H - H_2O]^-$ even at higher collision amplitudes, while CID in the HCD cell generally achieved a much larger variety of product ions, in particular at lower m/z values. These differences can be readily explained by the different modes of collision activation in the two different regions, i.e., selective resonance activation of the precursor ion in the LIT versus nonselective multiple collision activation in the HCD cell, in addition to low mass cutoff discrimination effects of the ion trap. These differences can be readily demonstrated for 5-HETE (see Figure A in the Supporting Information). The two highly abundant product ions m/z 301 and 257 were common in most HETEs and originate from small neutral losses of H_2O and $H_2O + CO_2$.[50,53] Importantly, abundant and more diagnostic fragment ions such as m/z 115 and 203 were formed primarily in the HCD cell through dissociation reactions close to the hydroxy group.[50,53] An interesting exception was seen for 20-HETE. Unlike the other investigated hydroxy fatty acids, 20-HETE did not exhibit a large number of structurally significant product ions in the MS/MS spectrum. For most HETEs (e.g., 5-, 8-, 9-, 11-, 12-, and 15-HETE) dissociation readily occurred by bond cleavage on either side of the hydroxy group after migration of the neighboring double bond, resulting in a large number of product ions. 20-HETE only showed dissociation at higher collision energies in the LIT instrument, originating from consecutive neutral losses of H_2O and ethylene $[M - H - H_2O - C_2H_4]^-$.[53]

These spectra, along with retention times and isotope distribution patterns from the full scan experiments, were used to tentatively identify eicosanoid species, which were then further confirmed with the aid of analytical reference standards where available. The procedure went as follows: Initially, the basic chemical lipid structure was predicted on the basis of a comparison of both MS/MS spectra and chromatographic behavior of the unknown compounds with those of selected reference standards from each of the lipid groups in Table 1. The product ions from MS/MS experiments of each unknown peak were classified according to one of three underlying fragmentation mechanisms: (1) product ions representing neutral loss of H_2O and CO_2; (2) product ions from cleavage of carbon−carbon bonds along the backbone; (3) product ions produced by combination of mechanisms 1 and 2. As mentioned above, fragment ions from C−C cleavages reveal more characteristic information for predicting the structure of these species than ions produced by loss of simple neutral molecules (H_2O and CO_2), which are common with most eicosanoids. In addition, the prediction accuracy was improved by considering the isotope patterns as well as the chromatographic behavior on a C_{18} reversed-phase separation column, as the retention times of eicosanoids are determined by the number and the position of hydroxy groups attached to the carbon backbone.

To assess the reproducibility of the retention times, retention time correction was performed on the mixed calibration standard. In general, a polynomial regression fitting approach based on spectral features present in the mixed standard samples was used for the correction approach. In these experiments, the mixed standards resulted in 87 peak groups fulfilling these criteria and were hence used for the retention time correction. Comparing the uncorrected and normalized data revealed that the maximum retention time deviation was within the range of 20 s, thus demonstrating the excellent stability of the chromatographic method.

For automated isotope matching between predicted and measured spectra, peak shapes, m/z differences, and peak ratios were considered. Since isotopic peaks exhibit similar peak shapes in the temporal domain, it is possible to use automated routines for detection. A correlation-based approach was used to identify the correlated extracted ion chromatograms at predefined mass differences in the temporal domain. To filter out potential artifacts, a correlation threshold of $r = 0.9$ was applied. We have demonstrated the applicability of this approach exemplarily for 11,12-EET, for which the correlation of the peak intensity of $[M - H]^-$ (m/z 319.22280) and the corresponding isotope (m/z 320.2320) is linear across the entire sample set investigated ($r^2 = 0.9888$, see Figure B in the Supporting Information). Isotope annotations for tentatively identified peaks were additionally checked manually.

An illustrative example for the identification process is shown in the final section below.

Quantitative Method Validation. The mass measurement accuracy in the full scan and MS/MS modes was initially determined using calibration standards as well as selected lipid compounds in biological samples, both for interday and for

(47) Hankin, J. A.; Wheelan, P.; Murphy, R. C. *Arch. Biochem. Biophys.* **1997**, *340*, 317–30.
(48) Margalit, A.; Duffin, K. L.; Isakson, P. C. *Anal. Biochem.* **1996**, *235*, 73–81.
(49) Yang, P.; Felix, E.; Madden, T.; Fischer, S. M.; Newman, R. A. *Anal. Biochem.* **2002**, *308*, 168–77.
(50) Murphy, R. C.; Barkley, R. M.; Zemski Berry, K.; Hankin, J.; Harrison, K.; Johnson, C.; Krank, J.; McAnoy, A.; Uhlson, C.; Zarini, S. *Anal. Biochem.* **2005**, *346*, 1–42.
(51) Waugh, R. J.; Morrow, J. D.; Roberts, L. J., 2nd; Murphy, R. C. *Free Radical Biol. Med.* **1997**, *23*, 943–54.
(52) Wheelan, P.; Zirrolli, J. A.; Murphy, R. C. *Biol. Mass Spectrom.* **1993**, *22*, 465–73.
(53) Kerwin, J. L.; Torvik, J. J. *Anal. Biochem.* **1996**, *237*, 56–64.

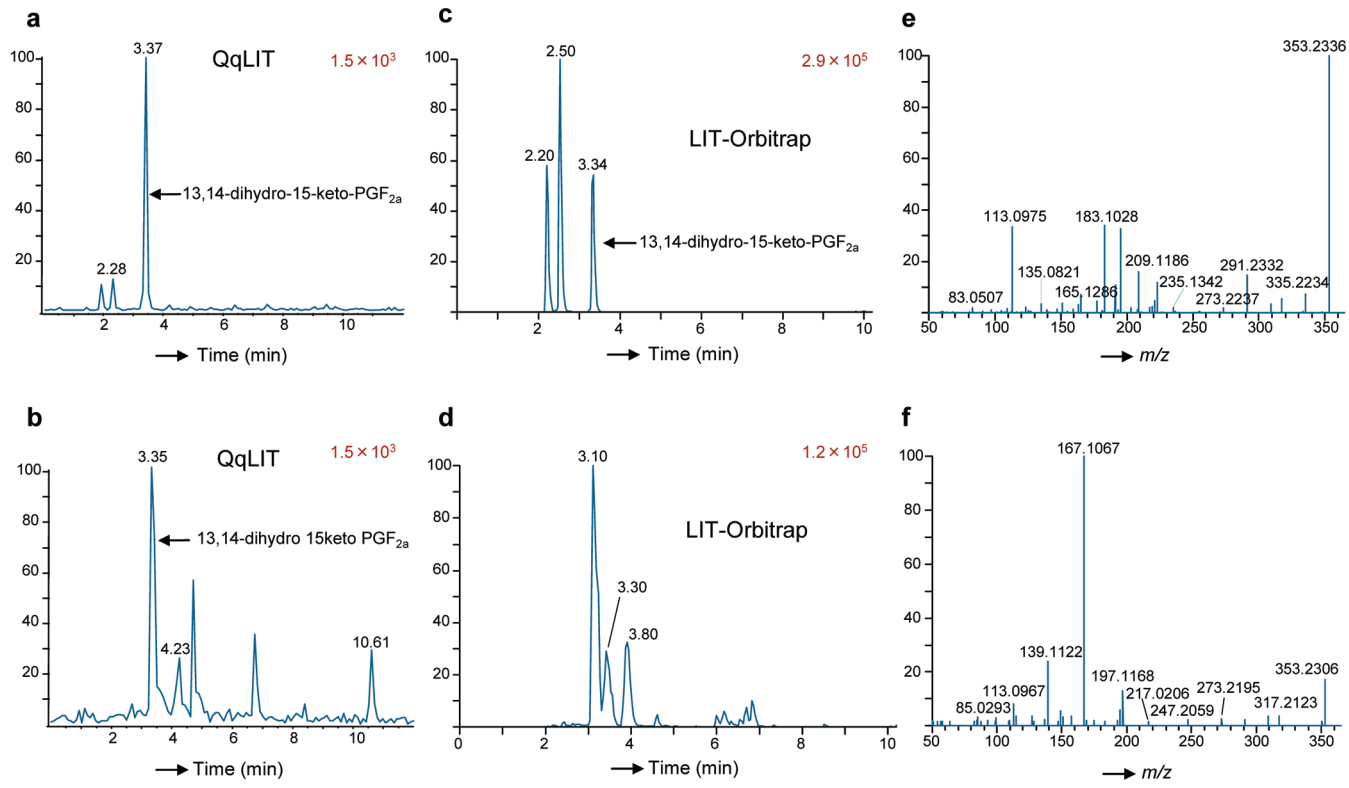

Figure 2. Identification of 13,14-dihydro-15-keto-$PGF_{2\alpha}$ using QqLIT (a, b) and orbitrap mass spectrometry (c−f): (a) QqLIT, 13,14-dihydro-15-keto-$PGF_{2\alpha}$ standard, MRM (*m/z* 353 → *m/z* 113); (b) QqLIT, 13,14-dihydro-15-keto-$PGF_{2\alpha}$, CLL sample, MRM (*m/z* 353 → *m/z* 113); (c) high-resolution extracted ion chromatogram, *m/z* 353.2335 of standard compounds; (d) high-resolution extracted ion chromatogram, *m/z* 353.2335 of the CLL sample; (e) corresponding MS/MS spectrum of the 13,14-dihydro-15-keto-$PGF_{2\alpha}$ standard; (f) corresponding MS/MS spectrum from the CLL sample. Spectra e and f demonstrate the false positive identification result of the QqLIT analysis.

intraday performance (see the table in the Supporting Information). Extracted MS/MS spectra were taken from the peak top and peak base to examine the mass accuracy across the full width of the chromatographic peak. The variation across the peaks was very small (<3.4 ppm in the full scan mode and <1.1 ppm in MS/MS experiments; see the Supporting Information), which was very important for identification and quantification purposes. This was particularly important for coeluting isomers, which were quantified on the basis of isomer-specific product ions from MS/MS experiments.

After identification of the bioactive lipids in biological samples, our analytical strategy comprised a subsequent quantitation step using the LIT−orbitrap mass spectrometer. We assessed the orbitrap's ability for quantitative analyses by comparing the analytical figures of merit to those obtained on a triple-quadrupole−linear ion trap instrument in the MRM mode, which is usually considered the gold standard for quantitative mass spectrometry assays in biological matrixes.

Six batches of calibration solutions were used to determine recoveries, LODs, LOQs, and linear dynamic ranges for the identified compound in CLL cells (Table 2). Each of these batches incorporated a representative compound from the lipid classes listed in Table 1, including 5-oxo-ETE, 11-HETE, PGB_2, LTB_4, PGE_3, PGE_2, $PGF_{2\alpha}$, TXB_2, 15-deoxy-$\Delta^{12,14}$-PGJ_2, 17-HDHA, RvD_2, and 13-HODE. In addition, for quantitative analysis of the CLL cells, the tentatively identified bioactive lipid compounds were added to these mixtures.

The compound recoveries ranged from 84% to 112% for all tested compounds with measurement precisions of better than 15% RSD. These measurements gave a linear dynamic range of 10−1000 pg/μL. The correlation coefficients (r^2) in these experiments ranged from 0.9724 to 0.9999 for all calibration curves (Table 2). The same validation samples were subsequently reanalyzed on a hybrid QqLIT MS instrument operated in the MRM mode, and the resulting data were compared to the quantitative orbitrap results. The analytical figures of merit were found to be within the same range as those obtained on the orbitrap MS instrument. For example, the accuracy of the mean of measured concentrations ranged from 95% to 103% on the orbitrap MS instrument and from 97% to 107% on the hybrid quadrupole−linear ion trap instrument.

The determined LOQ values were within a range of 50−100 pg injected on-column with a precision of better than 15% and accuracy of >95%. The measurement precision was less than 15% over the concentration range of 10−1000 pg/μL.

As can be seen from this comparison, the quantitative performance of both instruments was very similar. Importantly, however, only the LIT−orbitrap instrument was able to obtain both MS and MS/MS data with high mass accuracy and resolving power, which minimizes the number of false positive identifications for these metabolites in a biological matrix. For example, when CLL samples (vide infra) were analyzed on the QqLIT system, 13,14-dihydro-15-keto-$PGF_{2\alpha}$ was monitored on the basis of the MRM transition of m/z 353 → m/z 113 and the retention time (t_R = 3.37 and 3.35 min for the standard solution and CLL sample, respectively; Figure 2a,b). The orbitrap MS/MS analysis (Figure 2c,d) of the same peak, however, revealed a false positive identification in the QqLIT assay. MS/MS experiments with high

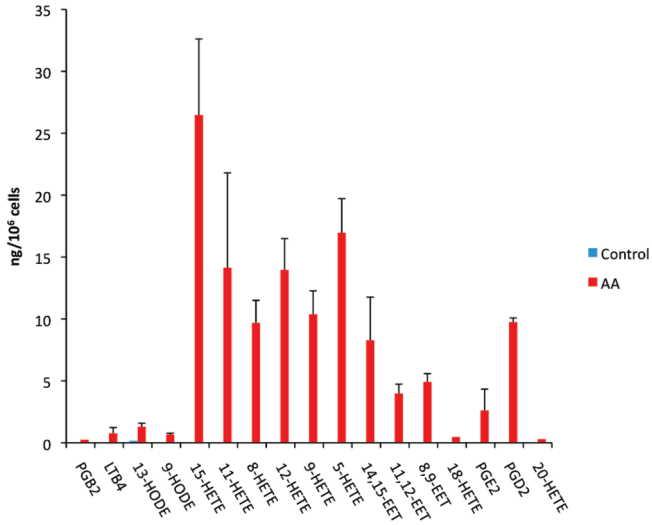

Figure 3. Profile of bioactive lipids in CLL cells over 24 h following supplementation with AA. The results are expressed as mean ± SEM ($n = 3$ subjects). Note that cells were isolated from different patients, thus explaining the large variation of the concentration levels.

mass accuracy on the orbitrap instrument confirmed the fragmentation pattern of this compound in biological samples to be different from the reference standard (Figure 2e,f).

Determination of Eicosanoid Profiles in CLL Cells. We applied our novel approach for a single-assay profiling of lipid mediators to the analysis of CLL cells. There are only very few studies on the endogenous levels of eicosanoids in CLL cells,[42,54] and to our knowledge, no study has shown a comprehensive eicosanoid profile due to previous limitations in analytical methodologies.

The production of lipid mediators is cell- and tissue-dependent. Therefore, to screen for all lipid mediators in CLL cells, we designed a pilot study in which these cells were stimulated with arachidonic acid (AA is the substrate for eicosanoids, Scheme 1) to test the applicability of our comprehensive assay.

The preliminary screening based on high-resolution MS and MS/MS data (vide supra) along with isotope pattern matching revealed the presence of 15 bioactive lipids, including PGB_2, LTB_4, 5-HETE, 8-HETE, 9-HETE, 11-HETE, 12-HETE, 15-HETE, 18-HETE, 20-HETE, 13-HODE, 14,15-EET, 11,12-EET, PGE_2, PGD_2, and 5-oxo-ETE. Figures 3 and 4 demonstrate the identification capabilities of the assay for profiling lipid mediators in CLL cells under basal conditions and following AA stimulation. A range of hydroxy and epoxy fatty acid lipid mediators were detected in supernatants of CLL cells (Figure 3). Some of these hydroxy fatty acids were detected at low levels in the negative control samples and were subtracted from the biological samples to determine the amounts produced in the presence of CLL cells (see Figure C in the Supporting Information).

The identification process is illustrated using 15-HETE as an example. 15-HETE was used as a reference compound (MW = 320.2350; see Table 1) to screen and identify related eicosanoids with identical exact mass. These related compounds were predicted on the basis of the relationships between the MS/MS spectra and structural features such as the position of functional groups, double bonds, and related product ions. For example, the MS/MS spectra of all candidate eicosanoids of MW = 320.2350 in CLL samples were compared to that of 15-HETE. Several product ions such as m/z 301 and 257 (loss of H_2O and $H_2O + CO_2$) were identical to 15-HETE, confirming the candidates' class association. Other product ions such as m/z 167, 155, 123, 115, and 179 were characteristic for the position of hydroxyl groups in the backbone and can be used to tentatively assign the candidate molecules to 11-HETE and 11,12-EET, 8-HETE, 9-HETE, 5-HETE and 12-HETE, respectively (Figure 4).

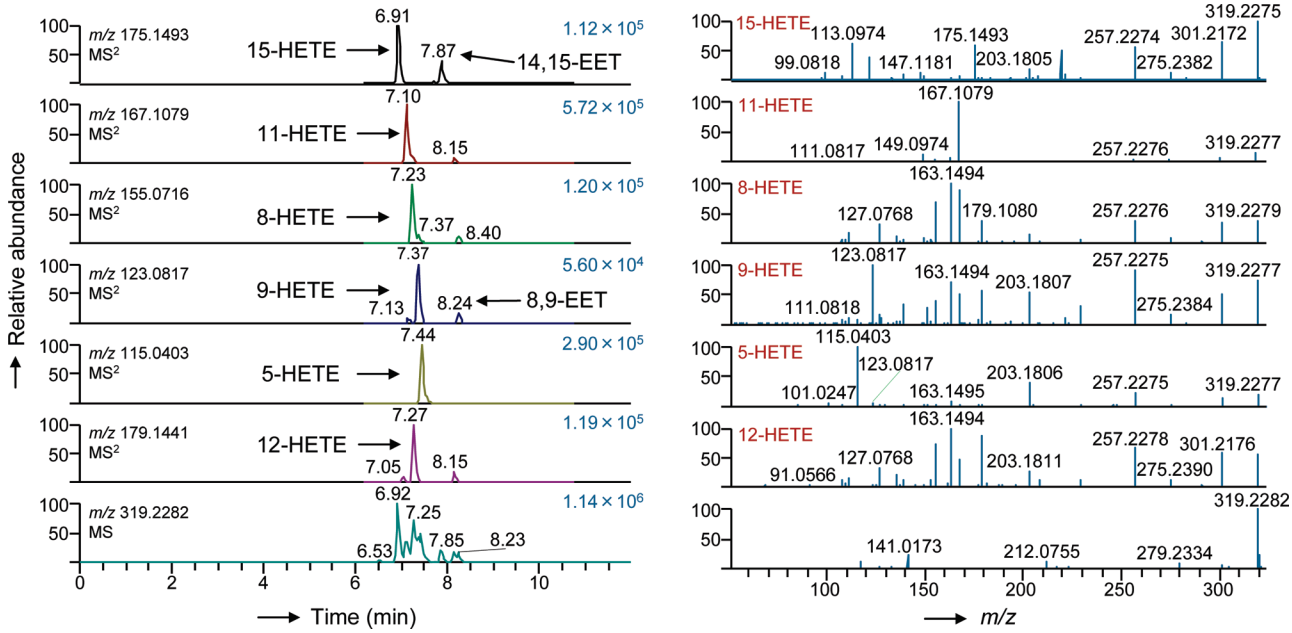

Figure 4. Identification of hydroxy and epoxy fatty acids in CLL cells following arachidonic acid supplementation: (a, left) extracted ion chromatograms using characteristic product ions; (b, right) corresponding CID spectra. Note that CID spectra are shown for the most abundant peak in the corresponding chromatograms, i.e., for $t_R = 6.91$, 7.10, 7.23, 7.44, 7.27, and 6.92 min (from top to bottom). The bottom trace shows the m/z 319 ion chromatogram extracted from the full scan trace and the corresponding full scan mass spectrum.

In addition, the retention behavior of these candidates on a reversed-phase C_{18} stationary phase further confirms these tentative assignments, as retention generally increases in reverse order compared to the number of hydroxyl groups. That is, trihydroxylated eicosanoids such as TXB_4 elute first, followed by the dihydroxylated species such as LTB_4, monohydroxylated eicosanoids, and finally nonoxidized fatty acids such as arachidonic acid. Also, epoxy fatty acids are eluted later than their related hydroxylated compounds; for example, 11-HETE and 11,12-EET eluted at 7.57 and 8.57 min in the chromatograms (see Figure 1) The concentration levels were subsequently determined by measuring the peak area ratios of characteristic product ions from the analyte and internal standard (PGB_2-d_4 or 12-HETE-d_8) and comparing them to the corresponding calibration curves. Calibration curves were calculated by least-squares linear regression.

Although this assay allows us to screen for a large number of bioactive lipids, we were not able to detect the enantiomers of HETE such as 12(*S*)-HETE and 12(*R*)-HETE or 15(*S*)-HETE and 15(*R*)-HETE, which could exhibit different physiological roles. The determination of these enantiomers requires chiral analysis as recently reported by Lee et al.[28]

CONCLUSIONS

In this paper we describe the development of an analytical technique for simultaneous profiling of over 100 biochemically related potent lipid mediators in biological samples. The technique provides a generic and comprehensive lipidomics approach for identification and quantitation of lipid mediators involved in important disease pathologies. A multistep procedure was implemented to extract eicosanoids from the biological matrix, chromatographically separate them using reversed-phase liquid chromatography, tentatively identify new candidate eicosanoids through matching retention times, isotope distribution patterns, and high-resolution MS/MS fragmentation patterns to representative group reference compounds, and quantify them by means of analytical reference standards. The method allowed us to examine eicosanoid profiles within the signaling cascade in CLL cells. The assay's sensitivity would readily allow transferring this method to other biological tissues.

Further improvements of this technique will focus on assay specificity, to confirm that the cyclooxygenase-derived products such as PGE_2 and PGD_2 can be inhibited using a nonselective cyclooxygenase inhibitor. In addition, chiral chromatography techniques for separation and identification of important stereoisomers within the biological cascade will be incorporated and a library of lipid mediators created, to accelerate and improve the identification process by using new algorithms for identifying potentially novel bioactive lipids in biological matrixes on the basis of MS, MS/MS, and retention behavior. Currently, these searches cannot be readily performed with the instrument manufacturers or other commercial software packages.

ACKNOWLEDGMENT

D.S. acknowledges funding from the Ontario Institute of Cancer Research (OICR; Grant No. 07Nov-61), the Canadian Institutes of Health Research (CIHR; Grant No. 190633), and the Leukemia and Lymphoma Society of Canada. D.A.V. acknowledges research support from the Medical Research Council (Cambridge Lipidomics Biomarker Research Initiative) and the Alfried Krupp von Bohlen und Halbach-Stiftung.

SUPPORTING INFORMATION AVAILABLE

Additional information as noted in the text. This material is available free of charge via the Internet at http://pubs.acs.org.

Received for review June 11, 2010. Accepted August 30, 2010.

AC1015563

(54) Hayden, R. E.; Pratt, G.; Davies, N. J.; Khanim, F. L.; Birtwistle, J.; Delgado, J.; Pearce, C.; Sant, T.; Drayson, M. T.; Bunce, C. M. *Leukemia* **2009**, *23*, 292–304.